

Meta-Learning across Meta-Tasks for Few-Shot Learning

Nanyi Fei¹ Zhiwu Lu¹ Yizhao Gao¹ Jia Tian¹ Tao Xiang² Ji-Rong Wen¹

Abstract

Existing meta-learning based few-shot learning (FSL) methods typically adopt an episodic training strategy whereby each episode contains a meta-task. Across episodes, these tasks are sampled randomly and their relationships are ignored. In this paper, we argue that the inter-meta-task relationships should be exploited and those tasks are sampled strategically to assist in meta-learning. Specifically, we consider the relationships defined over two types of meta-task pairs and propose different strategies to exploit them. (1) Two meta-tasks with disjoint sets of classes: this pair is interesting because it is reminiscent of the relationship between the source seen classes and target unseen classes, featured with domain gap caused by class differences. A novel learning objective termed meta-domain adaptation (MDA) is proposed to make the meta-learned model more robust to the domain gap. (2) Two meta-tasks with identical sets of classes: this pair is useful because it can be employed to learn models that are robust against poorly sampled few-shots. To that end, a novel meta-knowledge distillation (MKD) objective is formulated. Extensive experiments demonstrate that both MDA and MKD significantly boost the performance of a variety of FSL methods, resulting in new state-of-the-art on three benchmarks.

1. Introduction

Most object recognition models (especially those based on deep neural networks) require hundreds of labeled training samples from each object class. However, collecting and annotating large quantities of training samples is often infeasible or even impossible for certain classes in real-life scenarios (Antonie et al., 2001; Yang et al., 2012). One approach to addressing this challenge is few-shot learning

(FSL) (Li et al., 2003; 2006; Santoro et al., 2016a; Vinyals et al., 2016; Ravi & Larochelle, 2017; Finn et al., 2017), which aims to recognize a set of unseen classes with only few training samples by learning from a set of seen classes each containing ample samples.

Recently the FSL research has been dominated by meta-learning based methods (Finn et al., 2017; Snell et al., 2017; Sung et al., 2018; Ren et al., 2018; Chen et al., 2019a; Allen et al., 2019; Lee et al., 2019; Jamal & Qi, 2019). These methods typically adopt an episodic training strategy. In each episode, a meta-task is constructed by sampling N seen classes with few (K) shots as a support set and a separate query set of the same classes. Each meta-task is designed to simulate the N -way K -shot unseen class classification task. Across episodes, the meta-tasks are sampled randomly and independently. For each meta-task, a feature extractor and a classifier are learned: though the former is normally shared across tasks, the latter is learned whilst ignoring any relationships among the tasks. However, since these tasks are sampled from the same pool of seen classes, they are inevitably related in terms of the classes sampled (see Fig. 1(a)). In this paper, we propose to exploit the relationships between different tasks so that a model learned from seen classes can generalize better to unseen classes with only few training samples. In particular, we focus on exploring two types of inter-meta-task relationships and designing different learning objectives accordingly.

The first type is the one between two meta-tasks that have completely different sets of classes (see episodes $e^{(1)}$ and $e^{(3)}$ in Fig. 1(a)). This relationship is interesting because it is reminiscent of that between unseen and seen classes. Considering different tasks with different classes as domains, a key attribute of this relationship is the domain gap caused by class differences. Since an FSL model learned on seen classes needs to be adapted rapidly to unseen classes, this domain gap issue must be addressed. Joint learning over two such meta-tasks and introducing the domain adaptation (DA) learning objectives (Cortes et al., 2019; Zhang et al., 2019b; Rahman et al., 2020) across them thus enable the model to meta-learn how to be robust against the domain gap between unseen and seen classes. To this end, we introduce a DA loss over the two meta-tasks and name the resultant learning objective as meta-domain adaptation (MDA).

¹Beijing Key Laboratory of Big Data Management and Analysis Methods, Gaoling School of Artificial Intelligence, Renmin University of China, Beijing 100872, China. ²Department of Electrical and Electronic Engineering, University of Surrey, Guildford, Surrey GU2 7XH, United Kingdom. Correspondence to: Zhiwu Lu <luzhiwu@ruc.edu.cn>.

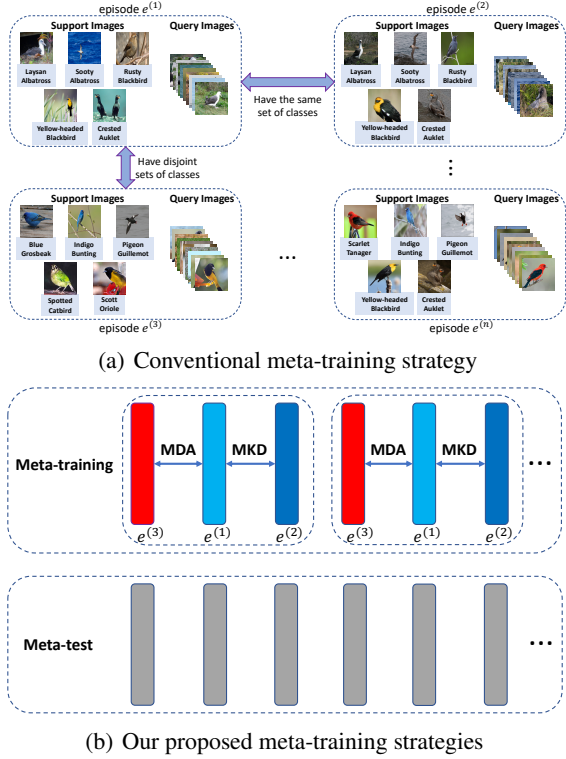


Figure 1. (a) Conventional meta-training strategy: episodes are sampled randomly and assumed to be independent even though they are inevitably related in terms of the classes sampled. Two types of relationships are of particular interest and shown here. (b) Our proposed meta-training strategy (including both MDA and MKD) with the conventional meta-test strategy: for each meta-training iteration, the red episode has a disjoint set of classes w.r.t. the two blue episodes, while the two blue episodes have the same set of classes (but with totally different samples).

The second type of inter-meta-task relationship is the one between two meta-tasks consisting of the same set of classes (see episodes $e^{(1)}$ and $e^{(2)}$ in Fig. 1(a)). We aim to take advantage of this relationship to address a specific challenge in few-shot learning, that is, how to learn a classifier with poorly sampled few training samples. Since each class is represented by only a handful of (K) samples, it is crucial for the model to be able to cope with outlying samples. In particular, with few samples per class, most existing FSL methods resort to very simple classifiers (e.g. the nearest neighbor classifier with each class represented as the sample mean adopted in prototypical networks (Snell et al., 2017)) which are sensitive to the sampling of training data. Given two meta-tasks of the same set of classes, it is now possible to enforce that the two classifiers learned with different support sets behave consistently. In other words, they should be insensitive to the random sampling of the data in the support sets. Inspired by knowledge distillation (Hinton et al., 2015), a novel meta-knowledge distillation (MKD) learning objective is formulated to enforce the consistency across the aforementioned two classifiers.

Armed with the MDA and MKD objectives for episodic training, a novel meta-training strategy termed meta-learning across meta-tasks (MLMT) is proposed, illustrated in Fig. 1(b). Specifically, we sample three meta-tasks in each training iteration, among which two contain the same set of seen classes (represented as the two blue episodes $e^{(1)}$ and $e^{(2)}$) and the third (represented as the red episode $e^{(3)}$) has a disjoint set of classes from the two blue episodes. With the three tasks, MKD is performed on $e^{(1)}$ to $e^{(2)}$ by enforcing classifier prediction consistency via knowledge distillation (Hinton et al., 2015) and MDA is applied between $e^{(3)}$ and $e^{(1)}/e^{(2)}$ via minimizing the domain adaptation loss (Zhang et al., 2019b). Once learned, we test the FSL model in the conventional way of meta-test as shown in Fig. 1(b).

Our contributions are three-fold: (1) For the first time, we propose to exploit the relationships across different meta-tasks explicitly for meta-learning. (2) We consider two types of relationships across FSL meta-tasks/episodes and propose two corresponding learning objectives (i.e., MDA and MKD) to address two key challenges faced by FSL: unseen-unseen domain gap caused by class differences, and poorly sampled few-shots. (3) Our proposed meta-learning strategy (i.e. MLMT) is applicable to most existing meta-learning based FSL methods (i.e., methods adopting episodic training). Extensive experiments demonstrate that these methods clearly benefit from MDA and MKD (see details in Sec. 4), resulting in new state-of-the-art performance.

2. Related Work

2.1. Few-Shot Learning

In recent years, most few-shot learning (FSL) approaches (Vinyals et al., 2016; Ravi & Larochelle, 2017; Finn et al., 2017; Snell et al., 2017; Sung et al., 2018; Mishra et al., 2018; Oreshkin et al., 2018; Qiao et al., 2018) are based on meta-learning with an episodic training strategy. These methods can be categorized into three groups: metric-based, model-based, and optimization-based. (1) Metric-based methods (Vinyals et al., 2016; Snell et al., 2017; Sung et al., 2018; Allen et al., 2019) try to learn a suitable metric for nearest neighbor search based classification. Instead of embedding all samples into a shared task-independent metric space, (Qiao et al., 2019) further learns an episodic-wise adaptive metric for classification. (2) Model-based methods (Santoro et al., 2016b; Munkhdalai & Yu, 2017) fine-tune their models trained on seen classes in order to quickly adapt them to unseen classes. (3) Optimization-based methods (Ravi & Larochelle, 2017; Finn et al., 2017; Li et al., 2017; Lee et al., 2019) exploit novel optimization algorithms instead of the standard gradient descent, again for quick adaptation from seen to unseen classes. Regardless which groups existing FSL methods belong to, they all ignore the relationships between the meta-tasks randomly sampled in different

episodes. To the best of our knowledge, there is only one exception – meta-transfer learning (Sun et al., 2019) randomly samples a batch of independent episodes, records the class with the lowest accuracy in each meta-task/episode, and re-samples ‘hard’ tasks from the set of recorded classes. Instead of hard task mining in (Sun et al., 2019), we deliberately construct meta-task pairs with either completely same or different classes, in order to meta-learn a model that is robust against both the domain gap caused by class differences and poorly sampled training data caused by only having few-shots per class.

2.2. Domain Adaptation

Domain adaptation (DA) (Pan et al., 2010; Cortes et al., 2019; Rahman et al., 2020) aims to reduce the domain gap between the source and target domains. Under the popular unsupervised DA setting (Gong et al., 2012; Ganin & Lempitsky, 2015), a large amount of labeled source data along with abundant unlabeled target data are provided. A number of recent DA works (Tzeng et al., 2017; Pinheiro, 2018; Long et al., 2018; Sohn et al., 2019; Zou et al., 2019; Zhang et al., 2019b; Chen et al., 2019b) are based on adversarial learning, which aligns the source and target distributions by reducing the domain gap in a minimax game. Under existing DA settings, the source and target domains are assumed to have the same set of classes. In our work, however, we aim to reduce the domain gap caused by disjoint sets of classes. This typically means larger data distribution discrepancy, which is harder to address with only few training samples.

Note that recently cross-domain FSL (Dong & Xing, 2018; Tseng et al., 2020) has started to draw attention, where the unseen classes in FSL are also from another problem domain (e.g., photo to sketch). Our work focuses on the conventional FSL setting but potentially can also be extended for the new cross-domain setting.

2.3. Knowledge Distillation

Knowledge distillation (KD) (Hinton et al., 2015) has become topical recently and several latest works have focused on KD with meta-learning (Flennerhag et al., 2019; Jang et al., 2019). Concretely, (Flennerhag et al., 2019) proposes a framework to transfer knowledge across learning processes, and (Jang et al., 2019) proposes a novel meta-learning approach to automatically learn what to transfer from the source network to the target network. Moreover, in meta-learning based FSL, Robust-dist (Dvornik et al., 2019) learns an ensemble of multiple networks and distills the ensemble into a single network to remove the overhead at test time. KD is also employed in our meta-knowledge distillation (MKD) learning objective. However, our objective is not to train a smaller target network more effectively, but to alleviate the effects of badly sampled support-sets.

3. Methodology

3.1. Problem Definition

Let \mathcal{C}_s denote a set of seen classes and \mathcal{C}_u denote a set of unseen classes, where $\mathcal{C}_s \cap \mathcal{C}_u = \emptyset$. We are then given a large sample set \mathcal{D}_s from \mathcal{C}_s , a few-shot sample set \mathcal{D}_u from \mathcal{C}_u , and a test set \mathcal{T} from \mathcal{C}_u , where $\mathcal{D}_u \cap \mathcal{T} = \emptyset$. Concretely, $\mathcal{D}_s = \{(x_i, y_i) | y_i \in \mathcal{C}_s, i = 1, \dots, N_s\}$, where x_i denotes the i -th image, y_i is the class label of x_i , and N_s denotes the number of images in \mathcal{D}_s . Similarly, the K -shot (i.e., each unseen class has K labeled images) sample set $\mathcal{D}_u = \{(x_i, y_i) | y_i \in \mathcal{C}_u, i = 1, \dots, N_u\}$, where $N_u = K|\mathcal{C}_u|$. The goal of FSL is to predict the labels of test images in \mathcal{T} by training a model with \mathcal{D}_s and \mathcal{D}_u .

3.2. Meta-Learning for FSL

Meta-learning based FSL methods (Vinyals et al., 2016; Finn et al., 2017; Snell et al., 2017; Sung et al., 2018; Lee et al., 2019) typically evaluate their models over unseen class classification meta-tasks (or episodes) sampled from \mathcal{C}_u . For meta-training, only the seen class samples in \mathcal{D}_s are used. An effective way to exploit the large sample set \mathcal{D}_s is to mimic the few-shot meta-test setting via episodic training. Specifically, to form an N -way K -shot Q -query episode $e = (\mathcal{S}_e, \mathcal{Q}_e)$, a subset \mathcal{C}_e of seen classes are first randomly sampled from \mathcal{C}_s , where $|\mathcal{C}_e| = N$. A support set $\mathcal{S}_e = \{(x_i, y_i) | y_i \in \mathcal{C}_e, i = 1, \dots, N \times K\}$ and a query set $\mathcal{Q}_e = \{(x_i, y_i) | y_i \in \mathcal{C}_e, i = 1, \dots, N \times Q\}$ ($\mathcal{S}_e \cap \mathcal{Q}_e = \emptyset$) are then generated by sampling K support images and Q query images from each class in the subset \mathcal{C}_e , respectively.

In this meta-learning framework, a typical FSL approach designs a few-shot classification loss for measuring the gap between the predicted labels and the ground-truth labels of the query set \mathcal{Q}_e over each episode e :

$$L_{cls}(e) = \mathbb{E}_{x \in \mathcal{Q}_e} L(y, h_{\Theta}(x; \mathcal{S}_e)), \quad (1)$$

where $L(\cdot, \cdot)$ is the classification loss, which is typically a cross-entropy loss, y is the ground-truth of x , and h_{Θ} can be any FSL model with a set of parameters Θ as long as it adopts episodic training. The FSL model h_{Θ} can be further represented as $h_{\Theta}(x; \mathcal{S}_e) = f(\psi(x); \mathcal{S}_e)$, where ψ denotes the feature extractor with an output feature dimension of d , and $f : \mathbb{R}^d \rightarrow \mathbb{R}^N$ denotes the scoring function constructed from \mathcal{S}_e within episode e . For conciseness, we replace $f(\psi(x); \mathcal{S}_e)$ with $f(\psi(x))$. The FSL model is then trained over the meta-training set by minimizing the loss function and is tested over the meta-test set.

3.3. Meta-Learning across Meta-Tasks (MLMT)

Existing meta-learning approaches described above take either one episode or a batch of episodes per training iteration and minimize loss functions defined within each episode independently, ignoring the underlying relations across dif-

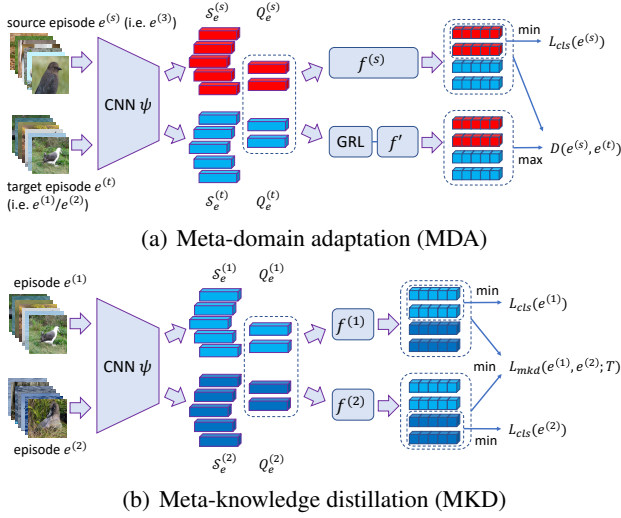


Figure 2. Schematic of our proposed meta-domain adaptation (MDA) and meta-knowledge distillation (MKD) objectives for meta-learning across meta-tasks (MLMT).

ferent meta-tasks. In contrast, with our meta-learning across meta-tasks (MLMT) strategy, three meta-tasks ($e^{(1)}$, $e^{(2)}$ and $e^{(3)}$) are sampled in each iteration, to have either identical ($e^{(1)}$ and $e^{(2)}$) or completely different sets of classes ($e^{(3)}$ to $e^{(1)}$ or $e^{(2)}$) among them. In this work, different learning objectives are then devised to exploit these two types of relationships (see Fig. 2).

3.3.1. META-DOMAIN ADAPTATION (MDA)

We consider $e^{(3)}$ as the source task, i.e., an $N^{(s)}$ -way $K^{(s)}$ -shot episode/task $e^{(s)} = (\mathcal{S}_e^{(s)}, \mathcal{Q}_e^{(s)})$ from $\mathcal{C}_e^{(s)} \subseteq \mathcal{C}_s$, and either $e^{(1)}$ or $e^{(2)}$ as the target task, which is an $N^{(t)}$ -way $K^{(t)}$ -shot episode $e^{(t)} = (\mathcal{S}_e^{(t)}, \mathcal{Q}_e^{(t)})$ from $\mathcal{C}_e^{(t)} \subseteq \mathcal{C}_s$, where $|\mathcal{C}_e^{(s)}| = N^{(s)}$, $|\mathcal{C}_e^{(t)}| = N^{(t)}$, and $\mathcal{C}_e^{(s)} \cap \mathcal{C}_e^{(t)} = \emptyset$. Note that since the two tasks are sampled from disjoint sets of classes, their number of ways or shots could be different.

Let $f^{(s)} : \mathbb{R}^d \rightarrow \mathbb{R}^{N^{(s)}}$ denote the scoring function constructed from $\mathcal{S}_e^{(s)}$ within source episode $e^{(s)}$, which is decided by the meta-learning FSL model h_Θ . We first introduce an auxiliary scoring function $f' : \mathbb{R}^d \rightarrow \mathbb{R}^{N^{(s)}}$ sharing the same hypothesis space with $f^{(s)}$. Since $f^{(s)}$ is used to score each sample in $\mathcal{Q}_e^{(s)}$ on the $N^{(s)}$ classes of $\mathcal{C}_e^{(s)}$, f' is designed as a metric-learning network that computes the similarity scores of query-prototype pairs. We set f' to be a multi-layer perceptron (MLP) module (see its detailed architecture in Sec. 4.1) stacked after the absolute difference between a query sample and a source class prototype (i.e. the mean representation of support samples from this source class). Our MDA learning objective is formulated as:

$$\min_{\psi, f^{(s)}} L_{cls}(e^{(s)}) + \lambda_{mda} D(e^{(s)}, e^{(t)}), \quad (2)$$

$$\max_{f'} D(e^{(s)}, e^{(t)}), \quad (3)$$

where λ_{mda} is the trade-off coefficient between the few-shot classification loss $L_{cls}(e^{(s)})$ and the DA loss $D(e^{(s)}, e^{(t)})$. Many existing DA losses can be considered (see Table 2). In this work, the recent margin disparity discrepancy (MDD) (Zhang et al., 2019b) is employed. We then have:

$$\begin{aligned} L_{cls}(e^{(s)}) &= \mathbb{E}_{x^{(s)} \in \mathcal{Q}_e^{(s)}} L(y^{(s)}, h_\Theta(x^{(s)}; \mathcal{S}_e^{(s)})) \\ &= \mathbb{E}_{x^{(s)} \in \mathcal{Q}_e^{(s)}} L(y^{(s)}, f^{(s)}(\psi(x^{(s)}))), \end{aligned} \quad (4)$$

$$\begin{aligned} D(e^{(s)}, e^{(t)}) &= \text{disp}_{e^{(t)}}(f^{(s)}, f') - \gamma \text{disp}_{e^{(s)}}(f^{(s)}, f') \\ &= \mathbb{E}_{x^{(t)} \in \mathcal{Q}_e^{(t)}} L'(f^{(s)}(\psi(x^{(t)})), f'(\psi(x^{(t)}))) \\ &\quad - \gamma \mathbb{E}_{x^{(s)} \in \mathcal{Q}_e^{(s)}} L(f^{(s)}(\psi(x^{(s)})), f'(\psi(x^{(s)}))), \end{aligned} \quad (5)$$

where γ is a positive hyper-parameter, and $\text{disp}_{e^{(s)}}(f^{(s)}, f')$ and $\text{disp}_{e^{(t)}}(f^{(s)}, f')$ are the two margin disparities of the source and target episodes, respectively. We train f' to maximize the MDD between the two episodes in Eq. (3) and train $\psi, f^{(s)}$ to minimize the maximum MDD in Eq. (2). In this minimax manner, the domain gap between the two episodes caused by their disjoint sets of classes is reduced. Note that our MDA is specifically designed for solving the FSL problem, particularly the data distribution discrepancy caused by the source/target class difference. To this end, a metric-learning based auxiliary classifier is introduced. In contrast, both the targeted problem and formulation are different in the original MDD, since it assumes that the source and target domains have the same set of classes.

With the softmax function $\sigma_j(\mathbf{v}) \triangleq \frac{\exp(v_j)}{\sum_{j'=1}^k \exp(v_{j'})}$ ($\mathbf{v} \in \mathbb{R}^k$, $j = 1, \dots, k$), the loss $L(\cdot, \cdot)$ used in Eqs. (4)–(5) is the cross-entropy loss:

$$L(y^{(s)}, f^{(s)}(\psi(x^{(s)}))) = -\log[\sigma_{y^{(s)}}(f^{(s)}(\psi(x^{(s)})))], \quad (6)$$

$$\begin{aligned} L(f^{(s)}(\psi(x^{(s)})), f'(\psi(x^{(s)}))) \\ = -\sum_{j=1}^{N^{(s)}} \sigma_j(f^{(s)}(\psi(x^{(s)}))) \log[\sigma_j(f'(\psi(x^{(s)})))]. \end{aligned} \quad (7)$$

Similarly, the loss $L'(\cdot, \cdot)$ used in Eq. (5) is a modified cross-entropy loss:

$$\begin{aligned} L'(f^{(s)}(\psi(x^{(t)})), f'(\psi(x^{(t)}))) \\ = \sum_{j=1}^{N^{(s)}} \sigma_j(f^{(s)}(\psi(x^{(t)}))) \log[1 - \sigma_j(f'(\psi(x^{(t)})))], \end{aligned} \quad (8)$$

which was introduced in (Goodfellow et al., 2014) to ease the burden of vanishing or exploding gradients.

Note that in Eq. (8), although $x^{(t)} \in \mathcal{Q}_e^{(t)}$ does not belong to any class in $\mathcal{C}_e^{(s)}$, the similarity scores after softmax $\sigma_j(f^{(s)}(\psi(x^{(t)})))$ and $\sigma_j(f'(\psi(x^{(t)})))$ ($j = 1, \dots, N^{(s)}$) can be considered to come from distributions in an $N^{(s)}$ -dimensional space. That is also the reason why we use the binary cross-entropy loss in both Eq. (7) and Eq. (8). Moreover, since $f^{(s)}$ is determined by the meta-learning based

FSL method h_Θ and it may contain no learnable parameters (e.g. prototypical networks (Snell et al., 2017) use the negative Euclidean distance as the score), we cut off the gradients over $f^{(s)}$ in Eq. (5) and directly train the feature extractor ψ to minimize this discrepancy loss through a gradient reversal layer (GRL) (Ganin & Lempitsky, 2015). The schematic of our MDA is shown in Fig. 2(a).

3.3.2. META-KNOWLEDGE DISTILLATION (MKD)

As is shown in Fig. 2(b), we consider another type of relationship between two meta-tasks which are sampled from exactly the same set of classes but with different samples. Specifically, we are given two N -way K -shot Q -query episodes $e^{(1)} = (\mathcal{S}_e^{(1)}, \mathcal{Q}_e^{(1)})$ and $e^{(2)} = (\mathcal{S}_e^{(2)}, \mathcal{Q}_e^{(2)})$ (both from a subset $\mathcal{C}_e \subseteq \mathcal{C}_s$, where $|\mathcal{C}_e| = N$ and $e^{(1)} \cap e^{(2)} = \emptyset$). Our MKD learning objective computed over the two episodes is designed to transfer knowledge from a strong classifier to a weak one. Here a classifier learned from one of the two episodes is weak when its K shots in the support set are more negatively impacted by outlying samples.

Let $f^{(1)} : \mathbb{R}^d \rightarrow \mathbb{R}^N$ and $f^{(2)} : \mathbb{R}^d \rightarrow \mathbb{R}^N$ be the scoring functions of the two classifiers within the two episodes, respectively. We first define an indicator function $I(A)$:

$$I(A) \triangleq \begin{cases} 1, & \text{if } A, \\ 0, & \text{if not } A. \end{cases} \quad (9)$$

To determine which classifier (scoring function) is stronger, we compute the few-shot classification accuracies of the two classifiers on the merged queries from both episodes. Concretely, for $\mathcal{Q}_e^{(1,2)} = \mathcal{Q}_e^{(1)} \cup \mathcal{Q}_e^{(2)} = \{(x_i^{(1,2)}, y_i^{(1,2)}) | y_i^{(1,2)} \in \mathcal{C}_e, i = 1, \dots, 2NQ\}$, we have:

$$acc^{(1)} = \frac{1}{2NQ} \sum_{i=1}^{2NQ} I(y_i^{(1,2)} = \hat{y}_i^{(1)}), \quad (10)$$

$$acc^{(2)} = \frac{1}{2NQ} \sum_{i=1}^{2NQ} I(y_i^{(1,2)} = \hat{y}_i^{(2)}), \quad (11)$$

where $y_i^{(1,2)}$ denotes the ground-truth label of $x_i^{(1,2)}$, $\hat{y}_i^{(1)} = \arg \max_j \sigma_j(f^{(1)}(\psi(x_i^{(1,2)})))$, and $\hat{y}_i^{(2)} = \arg \max_j \sigma_j(f^{(2)}(\psi(x_i^{(1,2)})))$ ($j = 1, \dots, N$). The classifier with higher accuracy is thus considered to be the stronger one and subsequently used as the teacher for distillation. Without loss of generality, we assume that $f^{(1)}$ is stronger (i.e. $acc^{(1)} > acc^{(2)}$). Our MKD learning objective is then stated as:

$$\min_{\psi, f^{(1)}, f^{(2)}} L_{cls}(e^{(1)}) + L_{cls}(e^{(2)}) + \lambda_{mkd} L_{mkd}(e^{(1)}, e^{(2)}; T), \quad (12)$$

where λ_{mkd} denotes a hyper-parameter, $L_{cls}(e^{(1)})$ and $L_{cls}(e^{(2)})$ are respectively the few-shot classification losses

defined over $e^{(1)}$ and $e^{(2)}$, and $L_{mkd}(e^{(1)}, e^{(2)}; T)$ is the knowledge distillation loss that is defined with a temperature T as in (Hinton et al., 2015):

$$L_{mkd}(e^{(1)}, e^{(2)}; T) = \mathbb{E}_{x^{(1,2)} \in \mathcal{Q}_e^{(1,2)}} L(f^{(1)}(\psi(x^{(1,2)})), f^{(2)}(\psi(x^{(1,2)})); T). \quad (13)$$

When the softmax function $\sigma_j(\mathbf{v}; T) \triangleq \frac{\exp(v_j/T)}{\sum_{j'=1}^k \exp(v_{j'}/T)}$ ($\mathbf{v} \in \mathbb{R}^k, j = 1, \dots, k$) is used for classification, we define $L(f^{(1)}(\psi(x^{(1,2)})), f^{(2)}(\psi(x^{(1,2)})); T)$ used in Eq. (13) with the following cross-entropy loss:

$$L(f^{(1)}(\psi(x^{(1,2)})), f^{(2)}(\psi(x^{(1,2)})); T) = - \sum_{j=1}^N \sigma_j(f^{(1)}(\psi(x^{(1,2)})); T) \log[\sigma_j(f^{(2)}(\psi(x^{(1,2)})); T)]. \quad (14)$$

3.4. MLMT-Based FSL Algorithm

As we have mentioned, in each training iteration, we randomly sample one $2N$ -way $2K$ -shot $2Q$ -query source episode/meta-task $e^{(s)} = (\mathcal{S}_e^{(s)}, \mathcal{Q}_e^{(s)})$ (i.e. $e^{(3)}$) and two N -way K -shot Q -query target episodes/meta-tasks $e^{(1)} = (\mathcal{S}_e^{(1)}, \mathcal{Q}_e^{(1)})$ and $e^{(2)} = (\mathcal{S}_e^{(2)}, \mathcal{Q}_e^{(2)})$. More specifically, the source episode has a disjoint set of classes w.r.t. either target episode (i.e. $\mathcal{C}_e^{(s)} \cap \mathcal{C}_e^{(1)} = \emptyset, \mathcal{C}_e^{(s)} \cap \mathcal{C}_e^{(2)} = \emptyset$), while the two target episodes must have exactly the same set of classes but different samples (i.e. $\mathcal{C}_e^{(1)} = \mathcal{C}_e^{(2)}, e^{(1)} \cap e^{(2)} = \emptyset$).

In each training iteration, we first determine the stronger/teacher target episode to compute the MKD loss between the two target episodes. We then compute the MDA loss between the source episode and the stronger target episode. The total loss for MLMT is finally given by:

$$L_{total} = L_{cls}(e^{(s)}) + L_{cls}(e^{(t)}) + L_{cls}(e^{(o)}) + \lambda_{mda} L_{mda}(e^{(s)}, e^{(t)}) + \lambda_{mkd} L_{mkd}(e^{(t)}, e^{(o)}; T), \quad (15)$$

where $e^{(t)} \in \{e^{(1)}, e^{(2)}\}$ denotes the stronger/teacher target episode, $e^{(o)} \in \{e^{(1)}, e^{(2)}\}$ denotes the other target episode, and $L_{mda}(e^{(s)}, e^{(t)}) = -D(e^{(s)}, e^{(t)})$. Note that minimizing L_{total} is actually equal to maximizing $D(e^{(s)}, e^{(t)})$. However, with the gradient reversal layer (GRL) between ψ and f' , we are still training ψ to minimize $D(e^{(s)}, e^{(t)})$.

It is worth pointing out that, when computing the MKD loss $L_{mkd}(e^{(t)}, e^{(o)}; T)$, we can even exploit the queries from $e^{(s)}$ to further improve the generalization ability of MKD. Although samples in $\mathcal{Q}_e^{(s)}$ do not belong to any class in $\mathcal{C}_e^{(t)}$ or $\mathcal{C}_e^{(o)}$, the two classifiers' outputs can still be aligned by minimizing the MKD loss, enforcing that they behave consistently even on the 'unseen' class data (i.e. $\mathcal{Q}_e^{(s)}$, unseen by them). A model learned with this MKD objective is thus more robust against the class-difference caused domain gap (i.e. seen classes to unseen ones) during meta-test, in addition to our MDA learning objective. Given

Algorithm 1 MLMT-Based FSL**Input:** Any meta-learning based FSL method h_Θ The seen class sample set \mathcal{D}_s Parameters $\lambda_{mda}, \lambda_{mkd}, \gamma, T$ **Output:** The learned h_Θ

- 1: **for all** iteration = 1, ..., MaxIteration **do**
- 2: Randomly sample one $2N$ -way $2K$ -shot source episode/meta-task $e^{(s)}$ (i.e. $e^{(3)}$) and two N -way K -shot target episodes/meta-tasks $e^{(1)}$ and $e^{(2)}$ from \mathcal{D}_s , satisfying that $\mathcal{C}_e^{(s)} \cap \mathcal{C}_e^{(1)} = \emptyset, \mathcal{C}_e^{(1)} = \mathcal{C}_e^{(2)}, e^{(1)} \cap e^{(2)} = \emptyset$;
- 3: Compute $L_{cls}(e^{(s)})$ with Eq. (4), and obtain $L_{cls}(e^{(1)}), L_{cls}(e^{(2)})$ in the same way;
- 4: Construct $\mathcal{Q}_e^{(1,2)} = \mathcal{Q}_e^{(1)} \cup \mathcal{Q}_e^{(2)}$ based on the two target episodes;
- 5: Compute $acc^{(1)}$ and $acc^{(2)}$ with Eq. (10) and Eq. (11), respectively;
- 6: **if** $acc^{(1)} > acc^{(2)}$ **then**
- 7: $t = 1; o = 2$;
- 8: **else**
- 9: $t = 2; o = 1$;
- 10: **end if**
- 11: Compute $D(e^{(s)}, e^{(t)})$ with Eq. (5), and obtain the MDA loss $L_{mda}(e^{(s)}, e^{(t)}) = -D(e^{(s)}, e^{(t)})$;
- 12: Construct $\mathcal{Q}_e^{(all)} = \mathcal{Q}_e^{(s)} \cup \mathcal{Q}_e^{(t)} \cup \mathcal{Q}_e^{(o)}$ based on the three episodes;
- 13: Compute the MKD loss $L_{mkd}(e^{(t)}, e^{(o)}; T)$ with Eq. (16);
- 14: Compute the total loss L_{total} with Eq. (15);
- 15: Compute the gradients $\nabla_{h_\Theta, f'} L_{total}$;
- 16: Update h_Θ, f' using stochastic gradient descent;
- 17: **end for**
- 18: **return** h_Θ .

$\mathcal{Q}_e^{(all)} = \mathcal{Q}_e^{(s)} \cup \mathcal{Q}_e^{(t)} \cup \mathcal{Q}_e^{(o)}$, we reformulate Eqs. (13)–(14) as follows:

$$\begin{aligned}
& L_{mkd}(e^{(t)}, e^{(o)}; T) \\
&= \mathbb{E}_{x^{(all)} \in \mathcal{Q}_e^{(all)}} L(f^{(t)}(\psi(x^{(all)})), f^{(o)}(\psi(x^{(all)})); T), \quad (16) \\
& L(f^{(t)}(\psi(x^{(all)})), f^{(o)}(\psi(x^{(all)})); T) \\
&= - \sum_{j=1}^N \sigma_j(f^{(t)}(\psi(x^{(all)})); T) \log[\sigma_j(f^{(o)}(\psi(x^{(all)})); T)].
\end{aligned} \quad (17)$$

By combining MDA and MKD learning objectives for episodic training, our MLMT-based FSL algorithm is summarized in Algorithm 1. Once learned, with the optimal FSL method h_Θ found by our algorithm, we randomly sample multiple N -way K -shot meta-test tasks from \mathcal{C}_u and average the top-1 test accuracies over these tasks as the final FSL results.

4. Experiments**4.1. Datasets and Settings**

Datasets. Three widely-used benchmark datasets are selected: (1) *miniImageNet*: This dataset (Vinyals et al., 2016) contains 100 classes from ILSVRC-12 (Russakovsky et al., 2015). Each class has 600 images. We split it into 64 training classes, 16 validation classes and 20 test classes as in (Ravi & Larochelle, 2017). (2) *tieredImageNet*: This dataset (Ren et al., 2018) is a larger subset of ILSVRC-12, which contains 608 classes and 779,165 images totally. As in (Ren et al., 2018), we split it into 351, 97, and 160 classes for training, validation, and test, respectively. (3) *CUB-200-2011 Birds (CUB)*: CUB (Wah et al., 2011) has 200 bird classes and 11,788 images in total. We split it into 100 training classes, 50 validation classes and 50 test classes as in (Chen et al., 2019a). All images of the three datasets are resized to 80×80 .

Evaluation Protocols. The 5-way 5-shot/1-shot settings are used. Each episode has 5 classes randomly sampled from the test split, which contains 5 shots (or 1 shot) and 15 queries per class. We thus have $N = 5, K = 5$ or $1, Q = 15$ for Algorithm 1 during meta-training as in previous works. We report the average 5-way few-shot classification accuracy (% , top-1) over 2,000 test episodes as well as 95% confidence interval.

Implementation Details. Our algorithm adopts Wide-ResNet-28-10 (WRN) (Zagoruyko & Komodakis, 2016) as the feature extractor ψ as in (Oreshkin et al., 2018; Qiao et al., 2018; Ye et al., 2018; Rusu et al., 2019), and the output feature dimension is 640. We pre-train WRN to accelerate the entire training process. The auxiliary scoring function f' used for our MDA strategy is formed by 4 fully-connected (FC) layers: {FC layer (640, 1024), batch normalization, ReLU, dropout(0.5)}, {FC layer (1024, 1024), ReLU, dropout(0.5)}, {FC layer (1024, 64), ReLU}, {FC layer (64, 1)}. The stochastic gradient descent (SGD) optimizer is employed with the initial learning rate of 1e-3 and the Nesterov momentum of 0.9. The learning rate is halved every 10 epochs. According to the validation performance of our algorithm, we uniformly set $\lambda_{mda} = 2, \lambda_{mkd} = 1, \gamma = 4$, and $T = 32$ over all datasets. The code and models will be released soon.

4.2. Main Results

Note that we can employ any meta-learning based FSL model as the baseline in Algorithm 1. In this work, without loss of generality, we apply our proposed meta-training strategy (i.e. MLMT) to three state-of-the-art FSL models: MetaOptNet (Lee et al., 2019), IMP (Allen et al., 2019), and FEAT (Ye et al., 2018). After adopting our meta-training strategy, each FSL model is thus named with the suffix

Table 1. Comparative results of conventional FSL on the three benchmark datasets. The average 5-way few-shot classification accuracies (% , top-1) along with 95% confidence intervals are reported on the test split of each dataset.

Method	Backbone	miniImageNet		tieredImageNet		CUB	
		1-shot	5-shot	1-shot	5-shot	1-shot	5-shot
MatchingNet (Vinyals et al., 2016)	Conv-4	43.56 \pm 0.84	55.31 \pm 0.73	-	-	-	-
Meta-LSTM (Ravi & Larochelle, 2017)	Conv-4	43.44 \pm 0.77	60.60 \pm 0.71	-	-	-	-
MAML (Finn et al., 2017)	Conv-4	48.70 \pm 1.84	63.11 \pm 0.92	51.67 \pm 1.81	70.30 \pm 1.75	71.29 \pm 0.95	80.33 \pm 0.70
ProtoNets (Snell et al., 2017)	Conv-4	49.42 \pm 0.78	68.20 \pm 0.66	53.31 \pm 0.89	72.69 \pm 0.74	71.88 \pm 0.91	87.42 \pm 0.48
RelationNet (Sung et al., 2018)	Conv-4	50.55 \pm 0.82	65.32 \pm 0.70	54.48 \pm 0.93	71.32 \pm 0.78	68.65 \pm 0.91	81.12 \pm 0.63
IMP (Allen et al., 2019)	Conv-4	49.60 \pm 0.80	68.10 \pm 0.80	-	-	-	-
SNAIL (Mishra et al., 2018)	ResNet-12	55.71 \pm 0.99	68.88 \pm 0.92	-	-	-	-
TADAM (Oreshkin et al., 2018)	ResNet-12	58.50 \pm 0.30	76.70 \pm 0.30	-	-	-	-
MTL (Sun et al., 2019)	ResNet-12	61.20 \pm 1.80	75.50 \pm 0.80	-	-	-	-
VariationalFSL (Zhang et al., 2019a)	ResNet-12	61.23 \pm 0.26	77.69 \pm 0.17	-	-	-	-
TapNet (Yoon et al., 2019)	ResNet-12	61.65 \pm 0.15	76.36 \pm 0.10	63.08 \pm 0.15	80.26 \pm 0.12	-	-
MetaOptNet (Lee et al., 2019)	ResNet-12	62.64 \pm 0.61	78.63 \pm 0.46	65.99 \pm 0.72	81.56 \pm 0.53	-	-
CAN (Hou et al., 2019)	ResNet-12	63.85 \pm 0.48	79.44 \pm 0.34	69.89 \pm 0.51	84.23 \pm 0.37	-	-
PPA (Qiao et al., 2018)	WRN	59.60 \pm 0.41	73.74 \pm 0.19	-	-	-	-
LEO (Rusu et al., 2019)	WRN	61.76 \pm 0.08	77.59 \pm 0.12	66.33 \pm 0.09	81.44 \pm 0.12	68.22 \pm 0.22	78.27 \pm 0.16
Robust-dist++ (Dvornik et al., 2019)	WRN	63.28 \pm 0.62	81.17 \pm 0.43	-	-	-	-
wDAE (Gidaris & Komodakis, 2019)	WRN	61.07 \pm 0.15	76.75 \pm 0.11	68.18 \pm 0.16	83.09 \pm 0.12	-	-
CC+rot (Gidaris et al., 2019)	WRN	62.93 \pm 0.45	79.87 \pm 0.33	70.53 \pm 0.51	84.98 \pm 0.36	-	-
S2M2 _R (Mangla et al., 2019)	WRN	64.93 \pm 0.18	83.18 \pm 0.11	-	-	80.68 \pm 0.81	90.85 \pm 0.44
MetaOptNet (Lee et al., 2019)	WRN	66.85 \pm 0.51	82.88 \pm 0.35	66.95 \pm 0.52	83.80 \pm 0.36	80.23 \pm 0.44	90.90 \pm 0.23
IMP (Allen et al., 2019)	WRN	69.50 \pm 0.50	83.19 \pm 0.35	67.45 \pm 0.53	81.93 \pm 0.38	79.53 \pm 0.46	89.34 \pm 0.27
FEAT (Ye et al., 2018)	WRN	70.13 \pm 0.49	82.48 \pm 0.35	68.71 \pm 0.55	84.04 \pm 0.35	81.89 \pm 0.41	90.66 \pm 0.23
MetaOptNet+MLMT (ours)	WRN	69.56 \pm 0.50	84.51 \pm 0.34	69.61 \pm 0.52	85.41 \pm 0.35	85.04 \pm 0.41	92.35 \pm 0.21
IMP+MLMT (ours)	WRN	71.35 \pm 0.49	84.96 \pm 0.34	69.40 \pm 0.52	84.60 \pm 0.37	82.62 \pm 0.44	91.12 \pm 0.25
FEAT+MLMT (ours)	WRN	72.41 \pm 0.49	84.34 \pm 0.33	72.82 \pm 0.52	85.97 \pm 0.35	85.23 \pm 0.40	92.53 \pm 0.22

‘+MLMT’ (e.g. MetaOptNet+MLMT). As described in Algorithm 1, we need to sample one $2N$ -way $2K$ -shot source episode and two N -way K -shot target episodes in each training iteration, which can be regarded as one $3N$ -way $2K$ -shot episode in total. For fair comparison, we thus re-implement MetaOptNet (Lee et al., 2019), IMP (Allen et al., 2019), and FEAT (Ye et al., 2018) by employing WRN as the backbone and sampling one $3N$ -way $2K$ -shot episode in each training iteration.

The comparative results on the three datasets are shown in Table 1. Models using the same backbones are placed together. ‘Conv-4’ denotes the simple feature extractor with only 4 convolutional blocks, which is widely used in previous works. We can make the following observations: (1) Models using WRN as the backbone generally outperform those adopting other feature extractors, showing that stronger feature extractor leads to better results. (2) Models trained with our MLMT strategy achieve new state-of-the-art on all three datasets. Importantly, the improvements over their original versions without using MLMT range from 1.4% to 4.8%. This clearly validates the effectiveness and general applicability of our MLMT for meta-learning based FSL. (3) The improvements obtained by our MLMT under the 1-shot setting are generally larger than those under the 5-shot setting. One plausible explanation is that: less support samples result in more unstable models (more prone to poorly data sampling when only one shot is sampled), and our meta-training objectives (particularly MKD) can alleviate such negative effects and thus achieve better results.

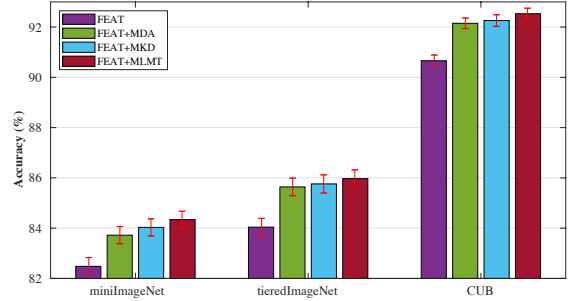


Figure 3. Ablative results for our full MLMT strategy (including both MDA and MKD) under the 5-way 5-shot setting. The error bars indicate the 95% confidence intervals.

4.3. Further Evaluation

Ablation Study. To demonstrate the contributions of each learning objective, we conduct ablative experiments with FEAT (Ye et al., 2018) as the baseline model under the 5-way 5-shot setting (more results under the 5-way 1-shot setting can be found in the suppl. material). The ablative results in Fig. 3 show that: (1) Adding MDA or MKD alone to the original FEAT clearly yields performance improvements (see FEAT+MDA vs. FEAT or FEAT+MKD vs. FEAT). MKD appears to be slightly more beneficial than MDA. (2) The combination of MDA and MKD (i.e. MLMT) achieves further improvements (see FEAT+MLMT vs. FEAT+MDA or FEAT+MLMT vs. FEAT+MKD), suggesting that our two learning objectives are complementary to each other.

Comparison to MDA and MKD Alternatives. We make comparison among different implementations of MDA and

Table 2. Comparison among different implementations of MDA on the test split of *miniImageNet*.

Method	1-shot	5-shot
FEAT	70.13 \pm 0.49	82.48 \pm 0.35
FEAT+MDA (CDAN)	71.07 \pm 0.50	83.57 \pm 0.35
FEAT+MDA (AFN)	71.22 \pm 0.50	82.84 \pm 0.35
FEAT+MDA (ours)	71.76 \pm 0.51	83.64 \pm 0.35

 Table 3. Comparison among different implementations of MKD on the test split of *miniImageNet*.

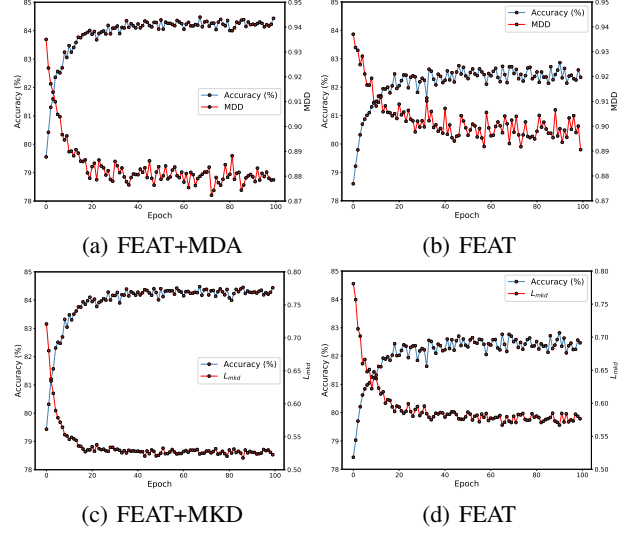
Method	EQ	1-shot	5-shot
FEAT	-	70.13 \pm 0.49	82.48 \pm 0.35
FEAT+MKD (symKL)	×	70.61 \pm 0.50	83.08 \pm 0.35
FEAT+MKD (symKL)	✓	71.78 \pm 0.50	83.67 \pm 0.35
FEAT+MKD (KD)	×	71.91 \pm 0.49	83.91 \pm 0.34
FEAT+MKD (KD)	✓	72.28 \pm 0.50	84.03 \pm 0.34

MKD in Table 2 and Table 3, respectively. Firstly, for MDA, we adopt CDAN (Long et al., 2018) and AFN (Xu et al., 2019) as alternative MDA implementations (in place of MDD in Eq. (5)). The obtained results in Table 2 show that the MDD loss is the best for MDA. With rigorous generalization bounds, MDD seems to have a marginal advantage over the alternatives when only few-shots per class are available. Secondly, for our MKD, we compare our asymmetric knowledge distillation loss (denoted as ‘KD’) in Eq. (17) to the symmetric KullbackLeibler (KL) divergence loss (denoted as ‘symKL’):

$$\begin{aligned}
 &L(f^{(t)}(\psi(x^{(all)})), f^{(o)}(\psi(x^{(all)})); T) \\
 &= \text{KL}(f^{(t)}(\psi(x^{(all)})), f^{(o)}(\psi(x^{(all)}))/T) \\
 &\quad + \text{KL}(f^{(o)}(\psi(x^{(all)})), f^{(t)}(\psi(x^{(all)}))/T), \quad (18)
 \end{aligned}$$

where $\text{KL}(\mathbf{p}, \mathbf{q}) = \sum_{j=1}^N \sigma_j(\mathbf{p}) \log \frac{\sigma_j(\mathbf{p})}{\sigma_j(\mathbf{q})}$ (\mathbf{p}, \mathbf{q} are two unnormalized N -dimensional scoring vectors). Note that we use query images from the source episode $e^{(s)}$ as external queries (denoted as ‘EQ’) when applying MKD over the two target episodes $e^{(t)}$ and $e^{(o)}$ in Algorithm 1. Therefore, we conduct additional experiments to study the effect of EQ. We can see from Table 3 that: (1) The asymmetric KD loss leads to better results than the symKL loss. (2) The external queries indeed can improve the performance of both KD and symKL, validating our detailed explanation above Eq. (16).

Visualization Results. We further provide the visualization of the generalization ability of our MDA and MKD during meta-test in Fig. 4 (more results during meta-validation can be found in the suppl. material). (1) **Visualization of MDA:** We randomly sample 1,000 episode pairs from the test split of *miniImageNet*, where the two 5-way 5-shot episodes in each pair have disjoint sets of classes. We compute the average 5-way classification accuracy over all 2,000 episodes and the average MDD over all 1,000 episode pairs at each training epoch. Note that we compute MDD using the original definition in (Zhang et al., 2019b) with our trained f' . We present the visualization results of FEAT+MDA


 Figure 4. Visualization of the generalization ability of our MDA and MKD on the test split of *miniImageNet* under the 5-way 5-shot setting. We check the test performance of the learned models at each training epoch.

and FEAT in Fig. 4(a) and Fig. 4(b), respectively. We can observe that FEAT+MDA has higher accuracies and lower MDD values (i.e. smaller domain gap between two episodes) than FEAT. This provides direct evidence that our MDA learning objective can boost the generalization ability of the learned model during meta-test. (2) **Visualization of MKD:** We randomly sample 1,000 episode pairs, where the two 5-way 5-shot episodes in each pair have the same set of classes. Similarly, we compute the average accuracy over all 2,000 episodes and the average L_{mkd} in Eq. (13) over all 1,000 episode pairs at each training epoch. The visualization results in Fig. 4(c) and Fig. 4(d) show that FEAT+MKD has higher accuracies and lower L_{mkd} values (i.e. better performance consistency between two episodes) than FEAT. This provides further evidence that our MKD has a better generalization ability during meta-test.

5. Conclusions

We have investigated the problem of how to best sample training episodes given an existing meta-learning based FSL model in this paper. For the first time, we argue that the training episodes should not be sampled randomly. Instead, they should be sampled strategically to exploit two types of relationships across meta-tasks. Two learning objectives are then proposed for each relationship respectively. Extensive experiments demonstrate that our proposed MLMT strategy can boost existing episodic-training based FSL methods and achieve new state-of-the-art on three benchmark datasets. We hope that this work can inspire more studies on the relationship across different meta-tasks in a meta-learning framework, even beyond the FSL problem.

References

- Allen, K. R., Shelhamer, E., Shin, H., and Tenenbaum, J. B. Infinite mixture prototypes for few-shot learning. In *ICML*, pp. 232–241, 2019.
- Antonie, M.-L., Zaiane, O. R., and Coman, A. Application of data mining techniques for medical image classification. In *International Conference on Multimedia Data Mining*, pp. 94–101, 2001.
- Chen, W., Liu, Y., Kira, Z., Wang, Y. F., and Huang, J. A closer look at few-shot classification. In *ICLR*, 2019a.
- Chen, X., Wang, S., Long, M., and Wang, J. Transferability vs. discriminability: Batch spectral penalization for adversarial domain adaptation. In *ICML*, pp. 1081–1090, 2019b.
- Cortes, C., Mohri, M., and Medina, A. M. Adaptation based on generalized discrepancy. *Journal of Machine Learning Research (JMLR)*, 20(1):1–30, 2019.
- Dong, N. and Xing, E. P. Domain adaption in one-shot learning. In *ECML-PKDD*, pp. 573–588, 2018.
- Dvornik, N., Schmid, C., and Mairal, J. Diversity with co-operation: Ensemble methods for few-shot classification. In *ICCV*, pp. 3723–3731, 2019.
- Finn, C., Abbeel, P., and Levine, S. Model-agnostic meta-learning for fast adaptation of deep networks. In *ICML*, pp. 1126–1135, 2017.
- Flennerhag, S., Moreno, P. G., Lawrence, N. D., and Damianou, A. C. Transferring knowledge across learning processes. In *ICLR*, 2019.
- Ganin, Y. and Lempitsky, V. S. Unsupervised domain adaptation by backpropagation. In *ICML*, pp. 1180–1189, 2015.
- Gidaris, S. and Komodakis, N. Generating classification weights with GNN denoising autoencoders for few-shot learning. In *CVPR*, pp. 21–30, 2019.
- Gidaris, S., Bursuc, A., Komodakis, N., Perez, P., and Cord, M. Boosting few-shot visual learning with self-supervision. In *ICCV*, pp. 8059–8068, 2019.
- Gong, B., Shi, Y., Sha, F., and Grauman, K. Geodesic flow kernel for unsupervised domain adaptation. In *CVPR*, pp. 2066–2073, 2012.
- Goodfellow, I. J., Pouget-Abadie, J., Mirza, M., Xu, B., Warde-Farley, D., Ozair, S., Courville, A. C., and Bengio, Y. Generative adversarial nets. In *Advances in Neural Information Processing Systems*, pp. 2672–2680, 2014.
- Hinton, G. E., Vinyals, O., and Dean, J. Distilling the knowledge in a neural network. *CoRR*, abs/1503.02531, 2015.
- Hou, R., Chang, H., Ma, B., Shan, S., and Chen, X. Cross attention network for few-shot classification. In *Advances in Neural Information Processing Systems*, pp. 4005–4016, 2019.
- Jamal, M. A. and Qi, G.-J. Task agnostic meta-learning for few-shot learning. In *CVPR*, pp. 11719–11727, 2019.
- Jang, Y., Lee, H., Hwang, S. J., and Shin, J. Learning what and where to transfer. In *ICML*, pp. 3030–3039, 2019.
- Lee, K., Maji, S., Ravichandran, A., and Soatto, S. Meta-learning with differentiable convex optimization. In *CVPR*, pp. 10657–10665, 2019.
- Li, F., Fergus, R., and Perona, P. A bayesian approach to unsupervised one-shot learning of object categories. In *ICCV*, pp. 1134–1141, 2003.
- Li, F., Fergus, R., and Perona, P. One-shot learning of object categories. *IEEE Transactions on Pattern Analysis and Machine Intelligence (TPAMI)*, 28(4):594–611, 2006.
- Li, Z., Zhou, F., Chen, F., and Li, H. Meta-sgd: Learning to learn quickly for few shot learning. *CoRR*, abs/1707.09835, 2017.
- Long, M., Cao, Z., Wang, J., and Jordan, M. I. Conditional adversarial domain adaptation. In *Advances in Neural Information Processing Systems*, pp. 1647–1657, 2018.
- Mangla, P., Singh, M., Sinha, A., Kumari, N., Balasubramanian, V. N., and Krishnamurthy, B. Charting the right manifold: Manifold mixup for few-shot learning. *CoRR*, abs/1907.12087, 2019.
- Mishra, N., Rohaninejad, M., Chen, X., and Abbeel, P. A simple neural attentive meta-learner. In *ICLR*, 2018.
- Munkhdalai, T. and Yu, H. Meta networks. In *ICML*, pp. 2554–2563, 2017.
- Oreshkin, B., López, P. R., and Lacoste, A. Tadam: Task dependent adaptive metric for improved few-shot learning. In *Advances in Neural Information Processing Systems*, pp. 721–731, 2018.
- Pan, S. J., Tsang, I. W., Kwok, J. T., and Yang, Q. Domain adaptation via transfer component analysis. *IEEE Transactions on Neural Networks*, 22(2):199–210, 2010.
- Pinheiro, P. O. Unsupervised domain adaptation with similarity learning. In *CVPR*, pp. 8004–8013, 2018.

- Qiao, L., Shi, Y., Li, J., Wang, Y., Huang, T., and Tian, Y. Transductive episodic-wise adaptive metric for few-shot learning. In *ICCV*, pp. 3603–3612, 2019.
- Qiao, S., Liu, C., Shen, W., and Yuille, A. L. Few-shot image recognition by predicting parameters from activations. In *CVPR*, pp. 7229–7238, 2018.
- Rahman, M. M., Fookes, C., Baktashmotlagh, M., and Sridharan, S. On minimum discrepancy estimation for deep domain adaptation. In *Domain Adaptation for Visual Understanding*, pp. 81–94. Springer, 2020.
- Ravi, S. and Larochelle, H. Optimization as a model for few-shot learning. In *ICLR*, 2017.
- Ren, M., Triantafillou, E., Ravi, S., Snell, J., Swersky, K., Tenenbaum, J. B., Larochelle, H., and Zemel, R. S. Meta-learning for semi-supervised few-shot classification. In *ICLR*, 2018.
- Russakovsky, O., Deng, J., Su, H., Krause, J., Satheesh, S., Ma, S., Huang, Z., Karpathy, A., Khosla, A., Bernstein, M., Berg, A. C., and Fei-Fei, L. ImageNet large scale visual recognition challenge. *International Journal of Computer Vision (IJCV)*, 115(3):211–252, 2015.
- Rusu, A. A., Rao, D., Sygnowski, J., Vinyals, O., Pascanu, R., Osindero, S., and Hadsell, R. Meta-learning with latent embedding optimization. In *ICLR*, 2019.
- Santoro, A., Bartunov, S., Botvinick, M., Wierstra, D., and Lillicrap, T. Meta-learning with memory-augmented neural networks. In *ICML*, pp. 1842–1850, 2016a.
- Santoro, A., Bartunov, S., Botvinick, M., Wierstra, D., and Lillicrap, T. P. One-shot learning with memory-augmented neural networks. *CoRR*, abs/1605.06065, 2016b.
- Snell, J., Swersky, K., and Zemel, R. S. Prototypical networks for few-shot learning. In *Advances in Neural Information Processing Systems*, pp. 4080–4090, 2017.
- Sohn, K., Shang, W., Yu, X., and Chandraker, M. Unsupervised domain adaptation for distance metric learning. In *ICLR*, 2019.
- Sun, Q., Liu, Y., Chua, T.-S., and Schiele, B. Meta-transfer learning for few-shot learning. In *CVPR*, pp. 403–412, 2019.
- Sung, F., Yang, Y., Zhang, L., Xiang, T., Torr, P. H. S., and Hospedales, T. M. Learning to compare: Relation network for few-shot learning. In *CVPR*, pp. 1199–1208, 2018.
- Tseng, H.-Y., Lee, H.-Y., Huang, J.-B., and Yang, M.-H. Cross-domain few-shot classification via learned feature-wise transformation. In *ICLR*, 2020.
- Tzeng, E., Hoffman, J., Saenko, K., and Darrell, T. Adversarial discriminative domain adaptation. In *CVPR*, pp. 2962–2971, 2017.
- van der Maaten, L. and Hinton, G. Visualizing data using t-SNE. *Journal of Machine Learning Research*, 9:2579–2605, 2008.
- Vinyals, O., Blundell, C., Lillicrap, T., Kavukcuoglu, K., and Wierstra, D. Matching networks for one shot learning. In *Advances in Neural Information Processing Systems*, pp. 3630–3638, 2016.
- Wah, C., Branson, S., Welinder, P., Perona, P., and Belongie, S. The caltech-ucsd birds-200-2011 dataset. Technical Report CNS-TR-2011-001, California Institute of Technology, 2011.
- Xu, R., Li, G., Yang, J., and Lin, L. Larger norm more transferable: An adaptive feature norm approach for unsupervised domain adaptation. In *ICCV*, pp. 1426–1435, 2019.
- Yang, S., Bo, L., Wang, J., and Shapiro, L. G. Unsupervised template learning for fine-grained object recognition. In *Advances in Neural Information Processing Systems*, pp. 3122–3130, 2012.
- Ye, H., Hu, H., Zhan, D., and Sha, F. Learning embedding adaptation for few-shot learning. *CoRR*, abs/1812.03664, 2018.
- Yoon, S. W., Seo, J., and Moon, J. Tapnet: Neural network augmented with task-adaptive projection for few-shot learning. In *ICML*, pp. 7115–7123, 2019.
- Zagoruyko, S. and Komodakis, N. Wide residual networks. In *BMVC*, 2016.
- Zhang, J., Zhao, C., Ni, B., Xu, M., and Yang, X. Variational few-shot learning. In *ICCV*, pp. 1685–1694, 2019a.
- Zhang, Y., Liu, T., Long, M., and Jordan, M. I. Bridging theory and algorithm for domain adaptation. In *ICML*, pp. 7404–7413, 2019b.
- Zou, H., Zhou, Y., Yang, J., Liu, H., Das, H. P., and Spanos, C. J. Consensus adversarial domain adaptation. In *AAAI*, pp. 5997–6004, 2019.

APPENDIX

In this document, we provide more support results to show the effectiveness of our algorithm. Firstly, we show more ablative results on the three benchmark datasets under the 5-way 1-shot setting. Secondly, we give more visualization results of the generalization ability of our two learning objectives (i.e. MDA and MKD) during meta-validation. Finally, we show several examples of the data distribution of meta-tasks.

A. Ablative Results

Similar to the ablation study under the 5-way 5-shot setting in the main paper, we conduct additional experiments by introducing more learning objectives into FEAT (Ye et al., 2018) on the three benchmarks (i.e. *miniImageNet* (Vinyals et al., 2016), *tieredImageNet* (Ren et al., 2018), and CUB (Wah et al., 2011)) under the 5-way 1-shot setting. The ablative results in Fig. 5 show that: (1) Adding MDA or MKD alone to the original FEAT model clearly yields performance improvements (see FEAT+MDA vs. FEAT or FEAT+MKD vs. FEAT). It is also observed that MKD is slightly more beneficial than MDA. (2) The combination of MDA and MKD (i.e. our MLMT) achieves further improvements (see FEAT+MLMT vs. FEAT+MDA or FEAT+MLMT vs. FEAT+MKD), suggesting that our two learning objectives are complementary to each other for FSL.

B. Visualization Results

We provide more visualization results of the generalization ability of our two learning objectives (i.e. MDA and MKD) during meta-validation in Fig. 6.

Visualization of MDA. We randomly sample 1,000 episode pairs from the validation split of *miniImageNet*, where the two 5-way 5-shot episodes in each pair have disjoint sets of classes. We compute the average 5-way classification accuracy over all 2,000 episodes and the average MDD over all 1,000 episode pairs at each training epoch. We present the visualization results of FEAT+MDA and FEAT in Fig. 6(a) and Fig. 6(b), respectively. We can observe that FEAT+MDA has higher accuracies and lower MDD values (i.e. smaller domain gap between two episodes) than FEAT. This provides direct evidence that our MDA learning objective can boost the generalization ability of the learned model during meta-validation.

Visualization of MKD. We randomly sample 1,000 episode pairs, where the two 5-way 5-shot episodes in each pair have the same set of classes. Similarly, we compute the average accuracy over all 2,000 episodes and the average L_{mkd} over all 1,000 episode pairs at each training epoch. The visualization results in Fig. 6(c) and Fig. 6(d) show that

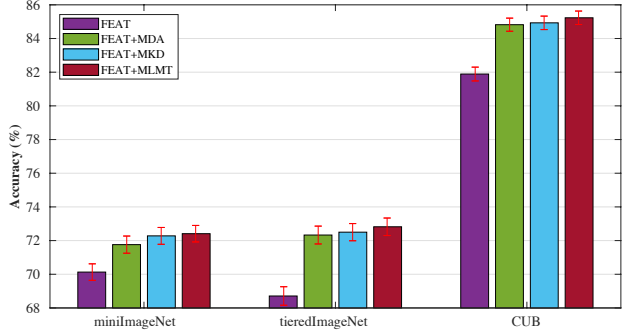


Figure 5. Ablative results for our full MLMT strategy (including both MDA and MKD) under the 5-way 1-shot setting. The error bars indicate the 95% confidence intervals.

FEAT+MKD has higher accuracies and lower L_{mkd} values (i.e. better performance consistency between two episodes) than FEAT. This provides further evidence that our MKD has a better generalization ability during meta-validation. Moreover, the results of FEAT+MKD after convergence have smaller variance than FEAT, which also validates that our MKD can help improve the model stability.

C. Qualitative Results

We further give qualitative results to show the effectiveness of our proposed MLMT. Concretely, we sample five meta-tasks in the test split of *miniImageNet* under the 5-way 5-shot setting and obtain the feature vectors of all images using CNNs trained with FEAT+MLMT and FEAT, respectively. We then apply t-SNE (van der Maaten & Hinton, 2008) to project these feature vectors into a 2-dimensional space in Fig. 7. In each small figure, samples with the same color belong to the same class. And two figures in each column represent the same meta-task. Similarly, we show the qualitative results in the test split of *miniImageNet* under the 5-way 1-shot setting in Fig. 8. We can observe that feature vectors obtained by FEAT+MLMT are generally more discriminative than FEAT, validating that our MLMT can help improve the generalization ability during meta-test.

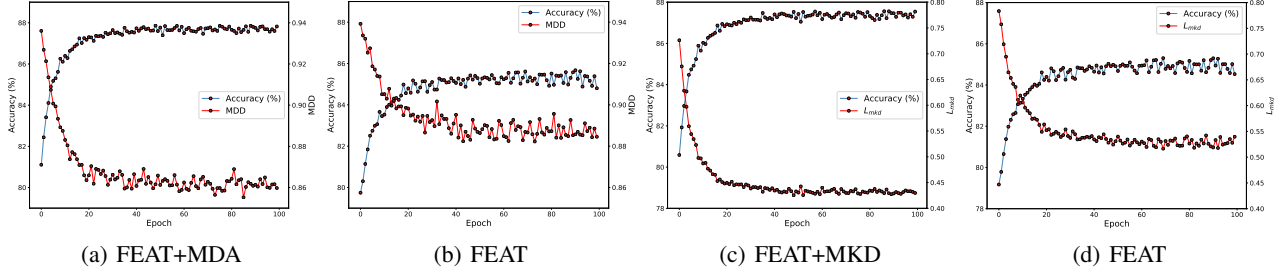


Figure 6. Visualization of the generalization ability of our learning objectives (i.e. MDA and MKD) on the validation split of *miniImageNet* under the 5-way 5-shot setting. Note that we check the validation performance of the learned models at each *training* epoch.

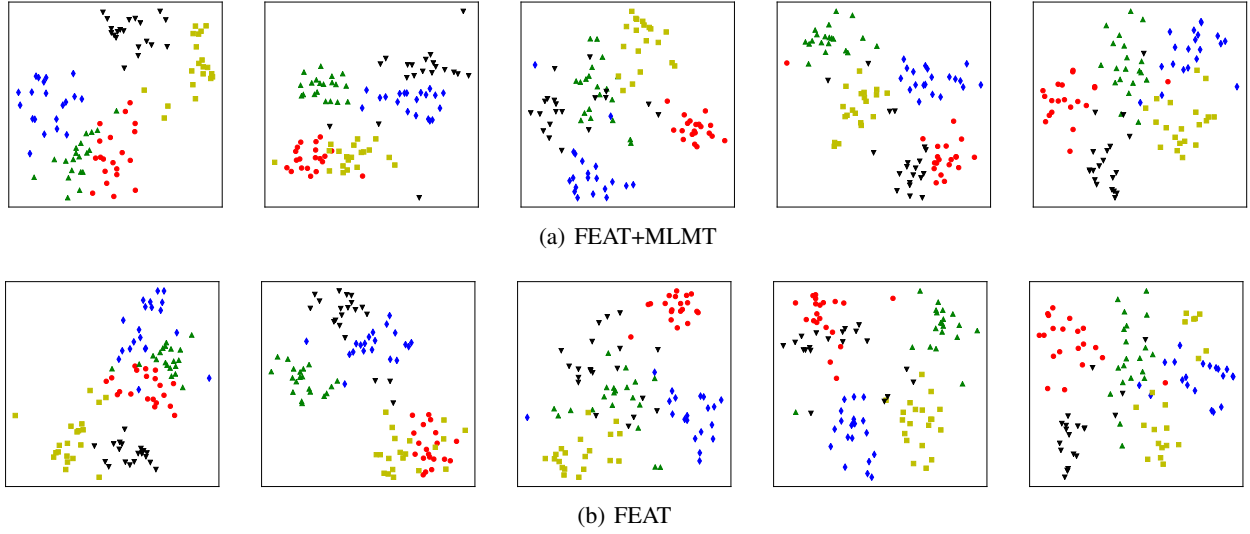


Figure 7. Examples of meta-tasks in the test split of *miniImageNet* under the 5-way 5-shot setting. In each small sub-figure, samples with the same color belong to the same class. The two sub-figures in each column represent the same meta-task.

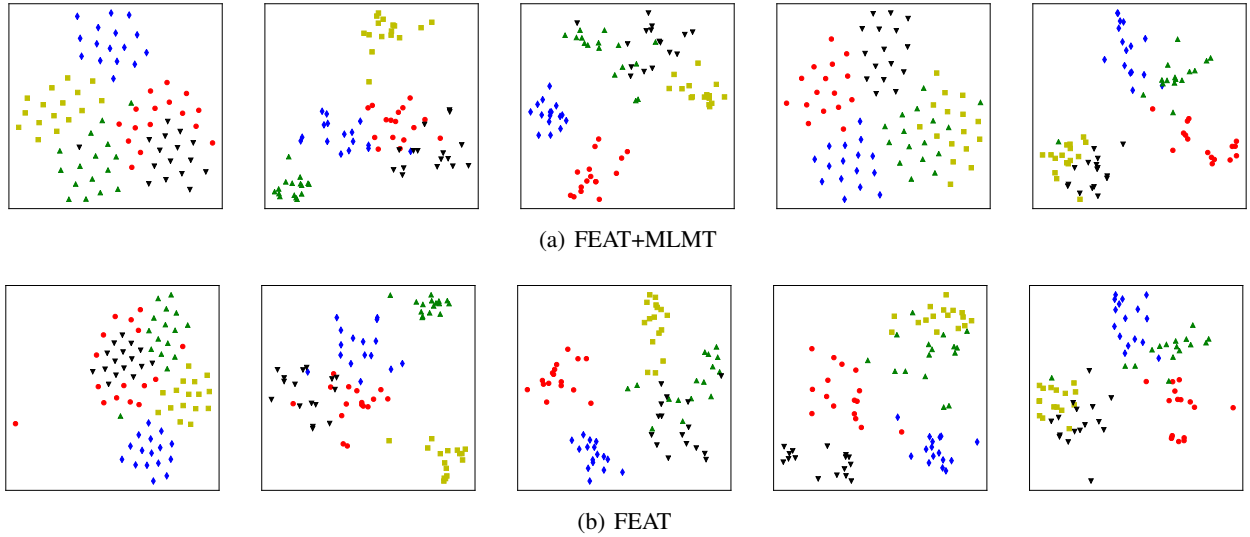


Figure 8. Examples of meta-tasks in the test split of *miniImageNet* under the 5-way 1-shot setting. In each small sub-figure, samples with the same color belong to the same class. The two sub-figures in each column represent the same meta-task.